

Final Ion-Charge Resolving Electron Spectroscopy: Photoionization Studies on Sm and Eu

T. Luhmann, Ch. Gerth, M. Martins, M. Richter, and P. Zimmermann

Institut für Strahlungs- und Kernphysik, Technische Universität Berlin, Hardenbergstrasse 36, 10623 Berlin, Germany

(Received 26 December 1995)

A new type of electron spectroscopy for the investigation of gas-phase targets has been developed. Based on electron-ion coincidence measurements using synchrotron radiation the method for the first time allows an electron spectrum to be split into the different final charge states. These spectra give deep insight into different, in part spin-dependent, multiple photoionization mechanisms, which is demonstrated for atomic samarium and europium in the photon energy range of the $4d$ giant resonances. [S0031-9007(96)00283-9]

PACS numbers: 32.80.Fb, 32.80.Hd

Photoionization studies of free atoms with monochromatized synchrotron radiation in the energy range of the vacuum ultraviolet (VUV) have been performed for more than thirty years to increase our knowledge about atomic structure and the dynamics of excitation and deexcitation processes. Besides photoabsorption experiments photoelectron and photoion spectroscopy have been established as versatile tools to investigate many-electron and relativistic effects ([1,2], and references therein). The combination of electron and ion spectroscopy, in particular, provides deep insight into the complexity of inner-shell photoprocesses since information about the first step of a photoionization decay process obtained by electron spectroscopy is related to information about the final ion-charge state obtained by ion spectroscopy. In this context an electron-ion coincidence experiment can be regarded as the most developed realization of such a combination [3–5]. This Letter presents this powerful method in its improved form where high coincidence counting rates are achieved which makes it possible for the first time to scan systematically a complete electron spectrum for fixed photon energy by electron-ion coincidence measurements. We call this new technique final ion-charge resolving electron spectroscopy (FIRE spectroscopy).

Our experiments were performed to study the complex excitation and decay processes of atomic Eu and Sm in the region of the $4d$ giant resonances. The atomic $4d$ giant resonances of the lanthanides are prominent examples for many-electron correlations in atoms, molecules, and solids ([2,6], and references therein). Moreover, this group of elements plays an important role in domains dealing with magnetism and/or (high temperature) superconductivity. In this context Eu is established as an important test case for many investigations because of its half-filled $4f$ subshell. The experimental setup is an improved version of an electron-ion coincidence apparatus used in previous investigations of atomic Ba [5]: Monochromatized synchrotron radiation of the electron storage ring BESSY in Berlin is focused onto an atomic beam of Eu or Sm. The photofragments are analyzed by a 180° cylindrical mirror electron analyzer and a time-of-flight ion spectrometer,

both equipped with microchannel plate (MCP) detectors. A detected electron with selected kinetic energy ε triggers a high voltage pulse which extracts the corresponding coincident photoion into the TOF spectrometer. In the resulting “coincidence-mode” ion spectrum, however, the spectrum of true coincidences is usually superimposed by the normal ion spectrum due to random coincidences, which is also measured, in a “reference mode,” by triggering the ion extraction pulses randomly using a pulse generator. Both coincidence-mode and reference-mode spectra are obtained almost simultaneously by switching between the two modes every 5 sec. From these two spectra the spectrum of true coincidences is calculated channel by channel, while correcting for (1) ion-detection efficiency of the ion MCP detector for different charge states, (2) dead-time effects due to the ion MCP detector and the corresponding pulse electronics, and (3) effects of event statistics of true and false coincidences in coincidence and reference mode [7]. Hence, our evaluation procedure takes into account all important effects of high counting rates. The total photoionization rate does not need to be reduced to avoid random coincidences but can be optimized to achieve best statistics of true coincidences in short accumulation time. In consequence, a great number of those measurements of different kinetic electron-energy values ε can be realized. The resulting spectra of true coincidences show directly the decay probabilities $p_{\hbar\omega}(\varepsilon, n+)$ for the decay to $n+$ after electron emission at different kinetic electron energy values ε for the chosen photon energy $\hbar\omega$. A FIRE spectrum $\text{EDC}_{\hbar\omega}^{n+}(\varepsilon)$ for fixed n and $\hbar\omega$ finally can be calculated by

$$\text{EDC}_{\hbar\omega}^{n+}(\varepsilon) = p_{\hbar\omega}(\varepsilon, n+)\text{EDC}_{\hbar\omega}(\varepsilon), \quad (1)$$

where $\text{EDC}_{\hbar\omega}(\varepsilon)$ denotes the measured electron spectrum (energy distribution curve) or a fitting curve to it. $\text{EDC}_{\hbar\omega}^{n+}(\varepsilon)$ represents the contribution of photoionization processes ending up in a $n+$ final state to the electron spectrum $\text{EDC}_{\hbar\omega}(\varepsilon)$ because

$$\begin{aligned} \sum_{n+} \text{EDC}_{\hbar\omega}^{n+}(\varepsilon) &= \left(\sum_{n+} p_{\hbar\omega}(\varepsilon, n+) \right) \text{EDC}_{\hbar\omega}(\varepsilon) \\ &= \text{EDC}_{\hbar\omega}(\varepsilon). \end{aligned} \quad (2)$$

As a first example Fig. 1 shows a fitting curve to a measured electron spectrum of atomic Eu ($[\text{Kr}]4d^{10}5s^25p^64f^76s^28S$) taken at 138.5 eV photon energy [$\text{EDC}_{\hbar\omega}(\epsilon)$, top] and its final ion-charge resolved contributions [$\text{EDC}_{\hbar\omega}^{n+}(\epsilon)$, $n = 1-4$] given on a kinetic electron energy scale (ϵ) as well as on an ionization energy scale ($I = \hbar\omega - \epsilon$). The data points were calculated according to Eq. (1). The error bars refer to the determination of the decay probabilities $p_{\hbar\omega}(\epsilon, n+)$ and are in most cases smaller than the data point symbols. The displayed fitting curves consist of a superposition of Gaussian profiles for photolines and a smooth background function, respectively. The position and width of the photoline profiles as obtained by the fit to the normal electron spectrum have not been varied during the fits to the FIRE spectra. The assignment of the photolines is based on a previous electron spectroscopy study [8]. The 1+ FIRE spectrum is dominated by the strong $4f^{-1}(^7F)$ photoline at

$I = 10.3$ eV accompanied by $4f^{-1}(^5F)$ photoemission structures at higher ionization energies ($I = 13-16$ eV) and a $6s^{-1}$ photoline at $I = 5.8$ eV. Whereas the energies of these hole states are located below the 2+ threshold at $I = 16.9$ eV, the $4f^{-1}6s^{-1}7s$ satellite process at $I = 17.5$ eV is able to end up in a 2+ final state by subsequent Auger decay which can be seen in the energy level diagram of Fig. 2. The complete absence of the corresponding photoline in the 1+ FIRE spectrum and a decay probability of 100% for a 2+ final state within the error bars indicates that charge conserving fluorescence decay into a 1+ final state as a competing process to Auger decay can be, indeed, neglected in the energy range of the VUV. This result has also been verified for the decay of the $5p^{-1}(^7,9P)$ hole states ($I = 26.7$ and 32.5 eV, respectively).

By the coincidence method it was also possible to determine and subtract the contribution of experimental background to the spectrum which does not result in true electron-ion coincidences. The remaining background in the spectra of Fig. 1, therefore, is due to direct double ionization processes where during one step two electrons are emitted simultaneously sharing

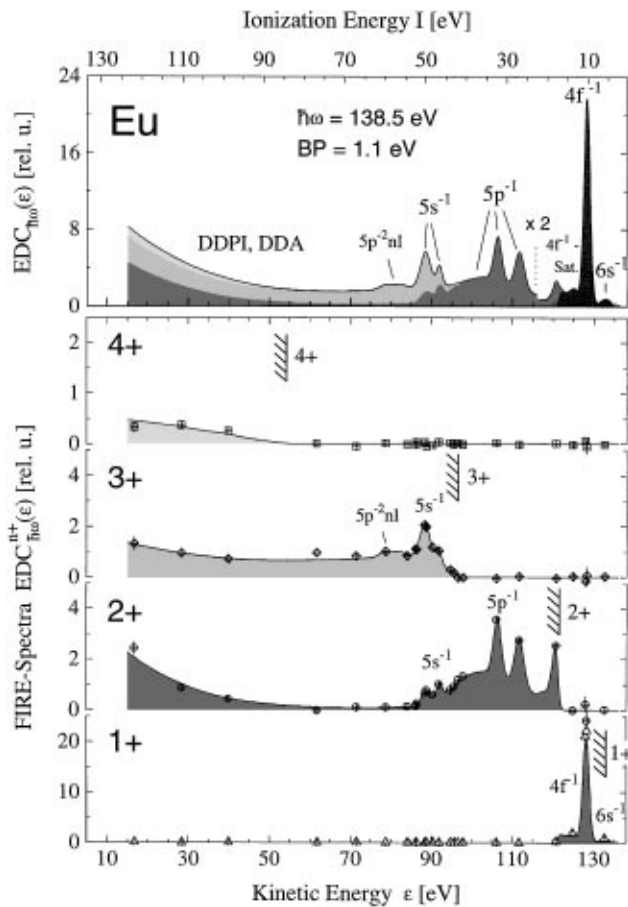


FIG. 1. Top: Fitting curve to a measured electron spectrum of atomic Eu taken at 138.5 eV photon energy. BP denotes the monochromator band pass. The different layers under the curve give the contributions of the different FIRE spectra. Below; FIRE spectra for the charge states Eu 1+ to 4+. The data points are obtained from Eq. (1) and are shown together with fitting curves. Ionization thresholds were taken from Ref. [9].

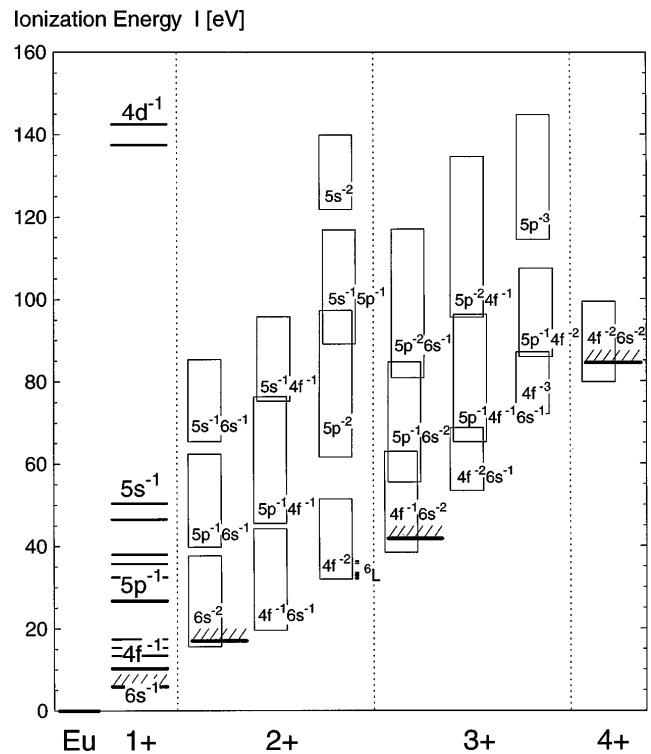


FIG. 2. Energy level scheme of Eu: $[\text{Kr}]4d^{10}5s^25p^64f^76s^2$. Energy levels of Eu 1+ were taken from Ref. [8], ionization thresholds of Eu 2+ to 4+ from Ref. [9]. Energy levels of Eu 2+ to 4+ surrounded by boxes were obtained by single configuration relativistic Hartree-Fock calculations using the Cowan code [10]. The number of levels contained in the boxes ranges between 198 levels for the configuration $4f^{-2}$ and 9448 levels for the configuration $5p^{-2}6s^{-1}$.

the available kinetic energy. In particular, the typically shaped electron background emission in the 2+ FIRE spectrum is explained by $(4f, 6s)^{-2}(\varepsilon\ell)_{\text{Ph1}}(\varepsilon\ell)_{\text{Ph2}}$ direct double photoionization (DDPI) without subsequent Auger decay, whereas the background in the 3+ FIRE spectrum can be explained by DDPI with subsequent Auger decay as well as by direct double Auger decay (DDA) after single photoionization [e.g., $4d^{-1} \rightarrow (4f, 6s)^{-3}(\varepsilon\ell)_{\text{Au1}}(\varepsilon\ell)_{\text{Au2}}$]. DDA after $4d^{-1}$ photoionization has been found to dominate the background emission in the electron spectra of atomic barium in the range of the $4d$ giant resonance [5]. By contrast, direct triple (or quadruple) ionization seems to be too exotic. The background in the 4+ FIRE spectrum of Fig. 1, therefore, should also be due to direct double ionization steps within a complete photoionization-decay cascade ending up in a 4+ final state.

$5s^{-1}$ single photoionization ($I = 43$ to 52 eV) is found to end up in a 2+ as well as in a 3+ final state (Fig. 1). Relativistic Hartree-Fock calculations using the Cowan code [10] show that $\text{Eu}^{3+}[\text{Xe}]4f^6$ states ($4f^{-1}6s^{-2}$) are extended to more than 10 eV above the $\text{Eu}^{3+}[\text{Xe}]4f^6 F_0$ threshold at $I = 41.8$ eV (Fig. 2). Hence, the stronger tendency of the $5s^{-1}7S$ photoionization process at higher ionization energy ($I = 50.4$ eV) for a decay to 3+ compared to the $5s^{-1}9S$ process ($I = 46.5$ eV) can be explained by the higher number of open Eu^{3+} decay channels. The weak structure in the 3+ spectrum at $I = 55$ to 63 eV is attributed to $5p^{-2}n\ell$ satellite emission followed by Auger decay.

The $4d^{-1}$ photoionization of Eu was studied at 168 eV photon energy. Figure 3 shows the corresponding electron and FIRE spectra. On the decay of $4d^{-1}$ hole states a 1+ final state was not observed within the error bars ($\leq 1\%$) indicating again the negligible role of charge conserving fluorescence decay. Based on a many-body perturbation theory calculation, the splitting of the Eu $4d^{-1}$ multiplet into two groups is explained by spin-orbit interaction of the $4d^{-1}$ hole [Eu: $4d_{3/2,5/2}^9 4f^7(^8S)^9D$] [8,11]. The existence of a corresponding 7D multiplet [Eu: $4d_{3/2,5/2}^9 4f^7(^8S)^7D$] has been predicted at ~ 20 eV higher ionization energy but has never been confirmed experimentally. However, the most interesting feature of the results in Fig. 3 is the complete suppression of the component at lower ionization energy ($I = 137.6$ eV) in the 2+ FIRE spectrum in contrast to the high ionization energy line group ($I = 142.5$ eV). This suggests a splitting due to spin coupling [$4d^9 4d^7(^8S)^7,9D$] even for the actual multiplet shown in Fig. 3. The reason is that the decay of a $4d^{-1}$ hole to 2+ is expected to be dominated by a $4d^{-1} \rightarrow 4f^{-2}(\varepsilon\ell)_{\text{Au}}(\varepsilon\ell)_{\text{Au}}$ Auger process [$4d^9 4f^7(^8S)^7,9D \rightarrow 4d^{10} 4f^5(^6L)(\varepsilon\ell)_{\text{Au}} 5,7L'$] because on the one hand the $4d$ - $4f$ overlap is large and on the other hand all the dominating Auger processes involving $5p$ electrons [$4d^{-1} \rightarrow 4f^{-1} 5p^{-1}(\varepsilon\ell)_{\text{Au}}$ and $4d^{-1} \rightarrow 5p^{-2}(\varepsilon\ell)_{\text{Au}}$] are able to

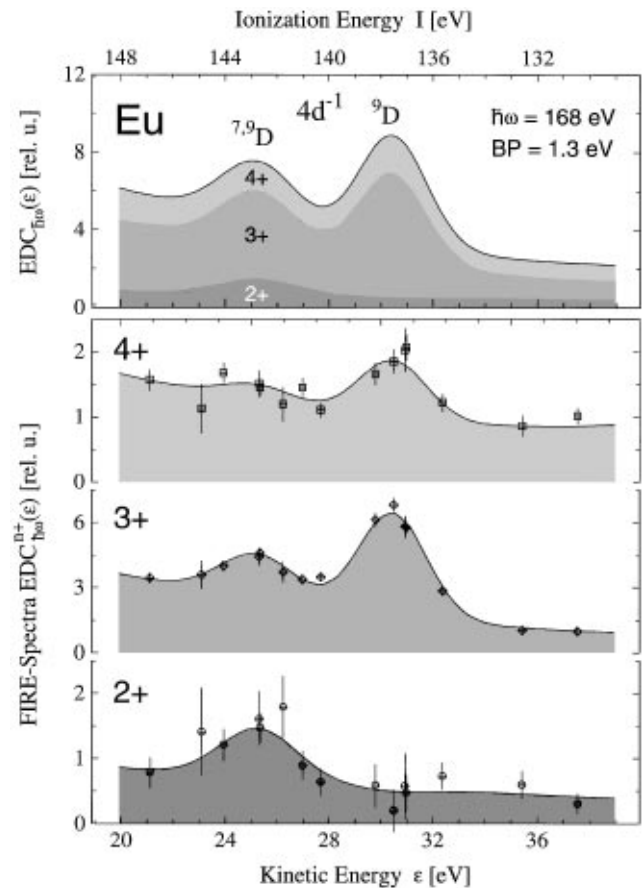


FIG. 3. Top: Fitting curve to a measured electron spectrum of atomic Eu taken at 168 eV photon energy in the range of the $4d^{-1}$ photolines. Below: FIRE spectra for the charge states Eu 2+ to 4+ (data points and fitting curves). Eu 1+ final charge states were not observed within the error bars and have been omitted for clarity. For further explanations see Fig. 1.

end up in a higher charged ion (see Fig. 2) [9,12]. A 9D spin coupling between the $4d^{-1}$ hole and the $4f$ shell would then imply a spin flip to $^5,7L'$ during the Auger decay which seems, indeed, not favorable and is forbidden in the LS coupling scheme.

The given explanation for the suppression of the $4d^{-1}$ line component in the 2+ FIRE spectrum of Fig. 3 is based on the fact that the spins of the seven electrons in the Eu $4f$ subshell are parallel (8S). To test this idea, therefore, Sm ($[\text{Kr}]4d^{10}5s^25p^64f^66s^2(^7F)$), one element before Eu in the periodic table, has also been investigated. Figure 4 shows the Sm $4d^{-1}$ multiplet by an electron spectrum taken at 158 eV photon energy and its final ion-charge resolved contributions. The Sm $4d^{-1}$ multiplet looks very similar to the Eu $4d^{-1}$ photoemission structure (Fig. 3) and exactly the same behavior concerning the decay to 2+ was observed: the complete suppression of the low ionization energy line component in the 2+ FIRE spectrum (Fig. 4).

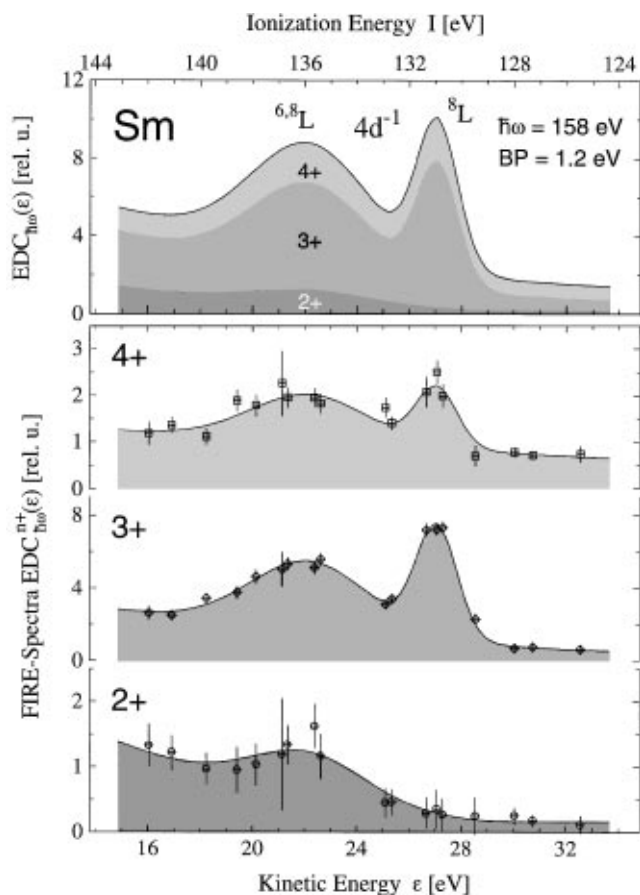


FIG. 4. Top: Fitting curve to a measured electron spectrum of atomic Sm taken at 158 eV photon energy in the range of the $4d^{-1}$ photolines. Below: FIRE spectra for the charge states Sm 2+ to 4+ (data points and fitting curves). Sm 1+ final charge states were not observed within the error bars and have been omitted for clarity. For further explanations see Fig. 1.

In conclusion, it can be summarized that a new type of electron spectroscopy (FIRE spectroscopy) has been

developed and applied to study many-electron decay on atomic Eu and Sm which in part has been found to be spin dependent. The experimental data allow an assignment for $4d^{-1}$ multiplet components to be given.

The authors thank the BESSY staff for assistance. The financial support of the Bundesministerium für Forschung und Technologie and the Deutsche Forschungsgemeinschaft is gratefully appreciated.

-
- [1] V. Schmidt, Rep. Prog. Phys. **55**, 1483 (1992).
 - [2] B. Sonntag and P. Zimmermann, Rep. Prog. Phys. **55**, 911 (1992).
 - [3] E. Shigemasa, T. Koizumi, Y. Itoh, T. Hayaishi, K. Okumo, A. Danjo, Y. Sato, and A. Yagishita, Rev. Sci. Instrum. **63**, 1505 (1992).
 - [4] B. Kämmerling, B. Krässig, and V. Schmidt, J. Phys. B **25**, 3621 (1992).
 - [5] S. Baier, G. Gottschalk, T. Kerkau, T. Luhmann, M. Martins, M. Richter, G. Snell, G. Snell, and P. Zimmermann, Phys. Rev. Lett. **72**, 2847 (1994).
 - [6] *Giant Resonances in Atoms, Molecules, and Solids*, edited by J.P. Connerade, J.M. Esteve, and R.C. Karnatak NATO Advanced Study Institutes (Plenum Press, New York, 1987).
 - [7] T. Luhmann, Rev. Sci. Instrum. (to be published).
 - [8] M. Richter, M. Meyer, M. Pahler, T. Prescher, E. v. Raven, B. Sonntag, and H.-E. Wetzel, Phys. Rev. A **40**, 7007 (1989).
 - [9] W.C. Martin, R. Zalubas, and L. Hagan, *Atomic Energy Levels—The Rare-Earth Elements* (U.S. Government Printing Office, Washington, D.C., 1978).
 - [10] R.P. Cowan, *The Theory of Atomic Structure and Spectra* (University of California Press, Berkeley, 1981).
 - [11] C. Pan, S.L. Carter, and H.P. Kelly, Phys. Rev. A **43**, 1290 (1991).
 - [12] M. Richter, T. Prescher, M. Meyer, E. v. Raven, B. Sonntag, H.E. Wetzel, and S. Aksela, Phys. Rev. B **38**, 1763 (1988).